ChemPubSoc Europe

DOI: 10.1002/cmdc.201200470

Exploring the Polyamine Regulatory Site of the NMDA Receptor: a Parallel Synthesis Approach

Michael L. Berger,*[a] Thomas Pöhler,[b] Oliver Schadt,[c] Maximilian Stanger,[a] Patrick Rebernik,[a] Petra Scholze,[a] and Christian R. Noe[b, c]

The elongated structures of polyamine inverse agonists such as 1,12-diaminododecane (N12N) and 5-(4-aminobutyl)-2-thiopheneoctanamine (N4T8N) lend themselves to a combinatorial chemistry approach to explore a potential polyamine pharmacophore at the NMDA receptor. Herein we describe more than 100 new analogues of N4T8N obtained by breaking up the long octanamine arm into a dipeptide chain of equivalent length. Solid-phase parallel synthesis based on cross-linked polystyrene and a Wang anchor allowed the low-scale preparation of four small libraries based on the combination of two amino acid residues (out of Gly, Leu, Phe, Lys, phenylglycine, Tyr, Trp, His, and Arg). The obtained compounds were tested as modulators of [^{3}H]MK-801 binding to rat brain membranes and of NMDA-induced currents in cultured rat hippocampal neurons. Compounds with two aromatic residues acted as binding inhibitors (inverse agonists). Compounds with two Lys residues acted as binding stimulators (agonists) and had stimulatory and inhibitory effects on NMDA-induced currents, depending on the holding potential. High sensitivity of binding inhibition to spermine was conferred by a Tyr residue, whereas a His residue favored high potency at acidic pH.

Introduction

A major success in drug discovery over the past 15 years has been the establishment of rapid and efficient high-throughput screening protocols to test compound libraries against multiple targets, endorsed by the advent of combinatorial chemistry yielding a variety of compounds during one cycle of synthesis.[1] Progress in solid-phase synthesis has revived interest in the chemical synthesis aspect of drug discovery. Several chemical reactions have been adapted or invented for this approach, and billions of compounds have been synthesized and screened by pharmaceutical companies. In contrast to compound mixtures obtained by classical combinatorial chemistry, the parallel synthesis approach, benefitting from progress in robotic technologies, provides compound libraries of known composition. The requirements and capacity of an academic research group led us and other research groups to elaborate a scheme for the differential screening of small libraries of compounds,[2] generating libraries of up to 50 compounds and taking advantage of the characteristic efficiency of solid-phase parallel synthesis. Individual compounds isolated from these libraries undergo pharmacological testing. Based on the results of these tests, structural optimization is achieved in an iterative interplay of library design and pharmacological testing. In view of the complexity in finding and developing a new drug, this approach appears superior to mass screening and is particularly suited for ligand profiling, as it affords more room for intellectual input from the individual experienced researcher.

We implemented this concept at the polyamine site of the NMDA receptor (NR). In contrast to the majority of binding assays, the binding procedure used allows discrimination between agonistic and antagonistic activities, because the affinity of the channel radioligand [^{3}H]MK-801[3] correlates with the frequency and duration of NR channel opening. We also tested two selected compounds in cultured hippocampal neurons. A C-amidated hexapeptide synthetic combinatorial library was tested at the NR by Ferrer-Montiel et al.;[4] Arg- and Trp-containing peptides turned out to be the most potent inhibitors. Another library of reduced peptidomimetic triamines was tested by Tai et al. at the NR,[5] returning compounds with aromatic substituents as the most potent inhibitors.

As late as the 1980s, excitation of NRs by Glu was considered to be a straightforward process that had evolved to maximize the rate of neuronal communication. However, several seminal discoveries during this decade demonstrated that Glu does not simply prompt this receptor to conduct cations into neurons, as is the case for acetylcholine at the neuromuscular junction. In 1983, Lodge and colleagues found that the dissociative anesthetics ketamine and phencyclidine act as blockers of NR channels.[6] In 1984, Ascher and co-workers discovered that NR channels are blocked by Mg^{2+} at sub-physiological concentrations,[7] and in 1986 it was demonstrated that the channel is highly permeable to Ca^{2+} ions.[8] In 1987, again the

[a] Dr. M. L. Berger, M. Stanger, P. Rebernik, Dr. P. Scholze
Center for Brain Research
Medical University of Vienna, 1090 Vienna (Austria)
E-mail: michael.berger@meduniwien.ac.at

[b] Dr. T. Pöhler, Prof. Dr. C. R. Noe
Pharmaceutical Chemistry, University of Vienna, 1090 Vienna (Austria)

[c] Dr. O. Schadt, Prof. Dr. C. R. Noe
Pharmaceutical Chemistry
Johann Wolfgang Goethe University, 60439 Frankfurt/Main (Germany)

Supporting information for this article is available on the WWW under http://dx.doi.org/10.1002/cmdc.201200470.

group of Ascher discovered glycine as the co-agonist at the NR.[9]

Maybe the scientific community was unwilling to accept additional breakthrough news regarding this receptor when in 1988 the first article to describe the stimulatory influence of other key molecules at this site was published: the ubiquitous polyamines spermidine and spermine were observed to increase [^{3}H]MK-801 binding to rat cortical membranes.[10] Electrophysiological corroboration of this phenomenon followed with some delay.[11] Thereafter, a debate on the possible significance of polyamines at the NR ensued, essentially between optimistic "bindologists" postulating a polyamine recognition site for agonists, inverse agonists and antagonists,[12] and sober, often skeptic physiologists, pointing to a complex multitude of actions,[13] both stimulatory and inhibitory. Cloning of the NRs in the early 1990s corroborated the physiological significance of polyamines for the NR, revealing an alternatively spliced cassette at the extracellular N-terminal domain of the essential subunit GluN1 with multiple positive charges,[14] mimicking the stimulatory influence of polyamines. Definite confirmation came recently, again from molecular biology studies[15] by which the polyamine stimulatory site was found to be localized at the interface between the N-terminal domains of subunits GluN1 and GluN2B. Our own studies began with a search for the optimum length of aliphatic long-chain diamines as inhibitors of [^{3}H]MK-801 binding,[16] culminating in the discovery of 5-(4-aminobutyl)-2-thiopheneoctanamine (N4T8N, $IC_{50} = 0.3\ \mu M$; **III** in Scheme 2 below),[17] formally equal to the medium potency inverse polyamine agonist 1,12-diaminododecane with asymmetric insertion of a thiophene nucleus. Further studies revealed increased sensitivity to spermine if an amide bond was inserted into the long arm of N4T8N.[18] Herein we present three libraries of compounds generated by parallel synthesis, an efficient synthetic approach for polyamines,[19] incorporating two amide bonds into the long arm of N4T8N.

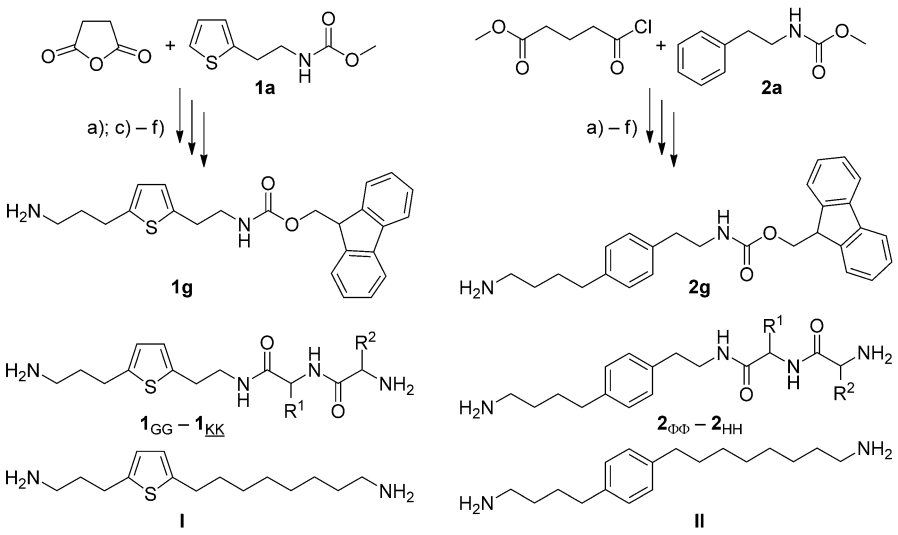

Scheme 1. Synthesis of the Fmoc-protected aminopropyl thienyl and aminobutyl phenyl building blocks, allowing solid-phase synthesis of $\mathbf{1}_{GG}$–$\mathbf{1}_{\underline{KK}}$ and $\mathbf{2}_{\underline{\Phi\Phi}}$–$\mathbf{2}_{HH}$, respectively, structurally related to the diamines **I** and **II**. *Reagents and conditions:* see Scheme 2.

Results and Discussion

Design and synthesis of dipeptidic polyamine analogues

Solid-phase synthesis allows low-scale preparation involving several steps without the need to isolate and purify the intermediates. These intermediates remain attached to a resin at a well-defined low density. We used polystyrene cross-linked by 1% divinylbenzene and modified by *para*-benzyloxybenzyl alcohol as anchor (a Wang anchor). The following starting building blocks were attached to this anchor: 1) for the first series, 5-(2-aminoethyl)-2-thiophenepropanamine (N3T2N) protected at the short aminoethyl arm with Fmoc (**1g** in Scheme 1), allowing solid-phase synthesis of the dipeptidic analogues N3T2N-aa$_1$-aa$_2$ $\mathbf{1}_{GG}$–$\mathbf{1}_{\underline{KK}}$; 2) for the second series, Fmoc-protected 4-(2-aminoethyl)-1-phenylbutanamine (N4h2N; **2g** in Scheme 1), resulting in analogues N4h2N-aa$_1$-aa$_2$ $\mathbf{2}_{\underline{\Phi\Phi}}$–$\mathbf{2}_{HH}$; and 3) for the third series, Fmoc-protected 5-(2-aminoethyl)-2-thiophenebutanamine (N4T2N; **3g** in Scheme 2), giving the analogues N4T2N-aa$_1$-aa$_2$ $\mathbf{3}_{\underline{\Phi\Phi}}$–$\mathbf{3}_{\underline{KK}}$ (Table 1). Thus, while permuting the amino acid residues, we also alternated between aminopropyl (series **1**) and aminobutyl (series **2** and **3**), and between thiophene (series **1** and **3**) and benzene (series **2**). Our previous data favored aminobutyl and thiophene,[17,18] but we were not sure if this would also hold for the dipeptidic analogues. As amino acid residues, we selected the aromatic Phe and the positively charged Lys based on promising observations,[4,5] and Gly and Leu for a simple comparison.

The conventional synthesis of the building blocks **1g**, **2g**, and **3g** (6–7 steps) is described in detail for **3g** only (Scheme 2). Analytical data for the routes leading to **1g** and **2g** are presented in the Supporting Information. To generate **3b**, the second alkyl substituent was introduced by Friedel–Crafts acylation with glutaric acid monomethyl ester chloride after protecting the amino group of the first substituent as methyl carbamate. The resulting ester **3b** was saponified, and the C=O group close to the thiophene ring was deoxygenated with Et_3SiH under acidic conditions. The protecting methyl carbamate was exchanged with Fmoc, the carboxylic group was converted into the amide, and the final amine **3g** was obtained by Hofmann rearrangement. Amides **1f** and **3f** were obtained in THF by adding NH_4HCO_3 after activating the carboxylic group with DCC and NHS. In the case of **2f**, the carboxylic group had to be converted into the acid chloride and reacted with gaseous ammonia (this step on the way to **2g** di-

Table 1. Compounds synthesized for the present study.[a]

Series **1**: H_2N-$(CH_2)_3$-2,5-thiophene-$(CH_2)_2$-NH-aa_1-aa_2

aa_1 \ aa_2	Gly	Leu	(D)-Leu	Phe	(D)-Phe	Lys	(D)-Lys
Gly	$\mathbf{1}_{GG}$	$\mathbf{1}_{GL}$	$\mathbf{1}_{G\underline{L}}$	$\mathbf{1}_{GF}$	$\mathbf{1}_{G\underline{F}}$	$\mathbf{1}_{GK}$	$\mathbf{1}_{G\underline{K}}$
Leu	$\mathbf{1}_{LG}$	$\mathbf{1}_{LL}$	$\mathbf{1}_{L\underline{L}}$	$\mathbf{1}_{LF}$	$\mathbf{1}_{L\underline{F}}$	$\mathbf{1}_{LK}$	$\mathbf{1}_{L\underline{K}}$
(D)-Leu	$\mathbf{1}_{\underline{L}G}$	$\mathbf{1}_{\underline{L}L}$	$\mathbf{1}_{\underline{L}\underline{L}}$	$\mathbf{1}_{\underline{L}F}$	$\mathbf{1}_{\underline{L}\underline{F}}$	$\mathbf{1}_{\underline{L}K}$	$\mathbf{1}_{\underline{L}\underline{K}}$
Phe	$\mathbf{1}_{FG}$	$\mathbf{1}_{FL}$	$\mathbf{1}_{F\underline{L}}$	$\mathbf{1}_{FF}$	$\mathbf{1}_{F\underline{F}}$	$\mathbf{1}_{FK}$	$\mathbf{1}_{F\underline{K}}$
(D)-Phe	$\mathbf{1}_{\underline{F}G}$	$\mathbf{1}_{\underline{F}L}$	$\mathbf{1}_{\underline{F}\underline{L}}$	$\mathbf{1}_{\underline{F}F}$	$\mathbf{1}_{\underline{F}\underline{F}}$	$\mathbf{1}_{\underline{F}K}$	$\mathbf{1}_{\underline{F}\underline{K}}$
Lys	$\mathbf{1}_{KG}$	$\mathbf{1}_{KL}$	$\mathbf{1}_{K\underline{L}}$	$\mathbf{1}_{KF}$	$\mathbf{1}_{K\underline{F}}$	$\mathbf{1}_{KK}$	$\mathbf{1}_{K\underline{K}}$
(D)-Lys	$\mathbf{1}_{\underline{K}G}$	$\mathbf{1}_{\underline{K}L}$	$\mathbf{1}_{\underline{K}\underline{L}}$	$\mathbf{1}_{\underline{K}F}$	$\mathbf{1}_{\underline{K}\underline{F}}$	$\mathbf{1}_{\underline{K}K}$	$\mathbf{1}_{\underline{K}\underline{K}}$

Series **2**: H_2N-$(CH_2)_4$-1,4-phenyl-$(CH_2)_2$-NH-aa_1-aa_2

aa_1 \ aa_2	(D)-PhG	Phe	Tyr	Trp	His
(D)-PhG	$\mathbf{2}_{\Phi\underline{\Phi}}$	$\mathbf{2}_{\Phi F}$	$\mathbf{2}_{\Phi Y}$	$\mathbf{2}_{\Phi W}$	$\mathbf{2}_{\Phi H}$
Phe	$\mathbf{2}_{F\underline{\Phi}}$	$\mathbf{2}_{FF}$	$\mathbf{2}_{FY}$	$\mathbf{2}_{FW}$	$\mathbf{2}_{FH}$
Tyr	$\mathbf{2}_{Y\underline{\Phi}}$	$\mathbf{2}_{YF}$	$\mathbf{2}_{YY}$	$\mathbf{2}_{YW}$	$\mathbf{2}_{YH}$
Trp	$\mathbf{2}_{W\underline{\Phi}}$	$\mathbf{2}_{WF}$	$\mathbf{2}_{WY}$	$\mathbf{2}_{WW}$	$\mathbf{2}_{WH}$
His	$\mathbf{2}_{H\underline{\Phi}}$	$\mathbf{2}_{HF}$	$\mathbf{2}_{HY}$	$\mathbf{2}_{HW}$	$\mathbf{2}_{HH}$

Series **3.1**: H_2N-$(CH_2)_4$-2,5-thiophene-$(CH_2)_2$-NH-aa_1-aa_2

aa_1 \ aa_2	(D)-PhG	Phe	Tyr	Trp	His
(D)-PhG	$\mathbf{3}_{\Phi\underline{\Phi}}$	$\mathbf{3}_{\Phi F}$	$\mathbf{3}_{\Phi Y}$	$\mathbf{3}_{\Phi W}$	$\mathbf{3}_{\Phi H}$
Phe	$\mathbf{3}_{F\underline{\Phi}}$	$\mathbf{3}_{FF}$	$\mathbf{3}_{FY}$	$\mathbf{3}_{FW}$	$\mathbf{3}_{FH}$
Tyr	$\mathbf{3}_{Y\underline{\Phi}}$	$\mathbf{3}_{YF}$	$\mathbf{3}_{YY}$	$\mathbf{3}_{YW}$	$\mathbf{3}_{YH}$
Trp	$\mathbf{3}_{W\underline{\Phi}}$	$\mathbf{3}_{WF}$	$\mathbf{3}_{WY}$	$\mathbf{3}_{WW}$	$\mathbf{3}_{WH}$
His	$\mathbf{3}_{H\underline{\Phi}}$	$\mathbf{3}_{HF}$	$\mathbf{3}_{HY}$	$\mathbf{3}_{HW}$	$\mathbf{3}_{HH}$

Series **3.2**: H_2N-$(CH_2)_4$-2,5-thiophene-$(CH_2)_2$-NH-aa_1-aa_2

aa_1 \ aa_2	Arg	His	(D)-Lys	Lys
Arg	$\mathbf{3}_{RR}$	$\mathbf{3}_{RH}$	$\mathbf{3}_{R\underline{K}}$	
His	$\mathbf{3}_{HR}$	$\mathbf{3}_{HH}$	$\mathbf{3}_{H\underline{K}}$	
(D)-Lys	$\mathbf{3}_{\underline{K}R}$	$\mathbf{3}_{\underline{K}H}$	$\mathbf{3}_{\underline{K}\underline{K}}$	$\mathbf{3}_{\underline{K}K}$

[a] Φ = (D)-PhG = (D)-phenylglycine; subscripts indicate single-letter code for amino acids (D isomers underlined).

verted from the steps leading to **1g** and **3g**; see the Supporting Information). The most difficult step was removal of the methyl carbamate protecting group from **3d**. We needed harsh basic conditions (Wolff–Kishner reduction) and achieved acceptable yields only by treating the raw product in situ with the Fmoc reagent.

To attach the generated building blocks **1g**, **2g**, and **3g** to the Wang anchor of the resin, the alcoholic residue of the anchor was activated with 4-nitrophenyl carbonate and 4-methylmorpholine.[20] The activated polymer was washed extensively and mixed with the hydroiodide or the trifluoroacetate of the mono-Fmoc-protected aromatic diamines **1g**–**3g**. After a short incubation period, the reaction mixture was alkalized to enable the coupling of the initial building blocks to the activated Wang anchor (Scheme 3). By this in situ strategy, the occurrence of side reactions was minimized.

After completion of the first coupling reaction and subsequent washing, the amino group was deprotected by treating the resin with 40% piperidine in DMF (Scheme 3, step b). The unprotected amino group can be readily converted into the corresponding amides in an initial diversification step using Fmoc-protected amino acids following the classical DIC/HOBt coupling protocol (step c).

With repeated cycles of deprotection and addition, any number of amino acids can be added to the resin (the technique had been originally designed for peptide synthesis). However, some amino acids bear reactive residues that would lend themselves as reaction partners in the described protocol. Six such amino acids were used in our libraries: Lys, (D)-Lys, Tyr, Trp, His, and Arg. The side chain nitrogen atoms in Lys, (D)-Lys, Trp, and His were protected by Boc, the side chain oxygen atom in Tyr with *O*-2-chlorotrityl, and the guanidine of Arg by 2,2,4,6,7-pentamethyl dihydrobenzofuran-5-sulfonyl (Pbf).[21] These orthogonal protecting groups are compatible with Fmoc deprotection under alkaline conditions and can be cleaved under acidic conditions in the final step of the described sequence. 1) If Tyr was present, the *O*-2-chlorotrityl protecting group was the first to be removed, with TFA in CH_2Cl_2; to scavenge liberated trityl cations, TIS was added.[22] 2) Next, the Fmoc protecting group was removed from the second amino acid with piperidine in DMF. 3) After extensive washing, the final product was cleaved from the resin and simultaneously deprotected from contingently present Boc or Pbf groups by incubating the resin with 95% TFA in CH_2Cl_2.

In vitro pharmacology

Effects of a single concentration

The synthesized dipeptidic polyamine analogues had diverse effects on [^{3}H]MK-801 binding to rat brain membranes. At 100 μM, most compounds of series **1** were ineffective at medium buffer concentration (50 mM Tris acetate, Figure 1A).

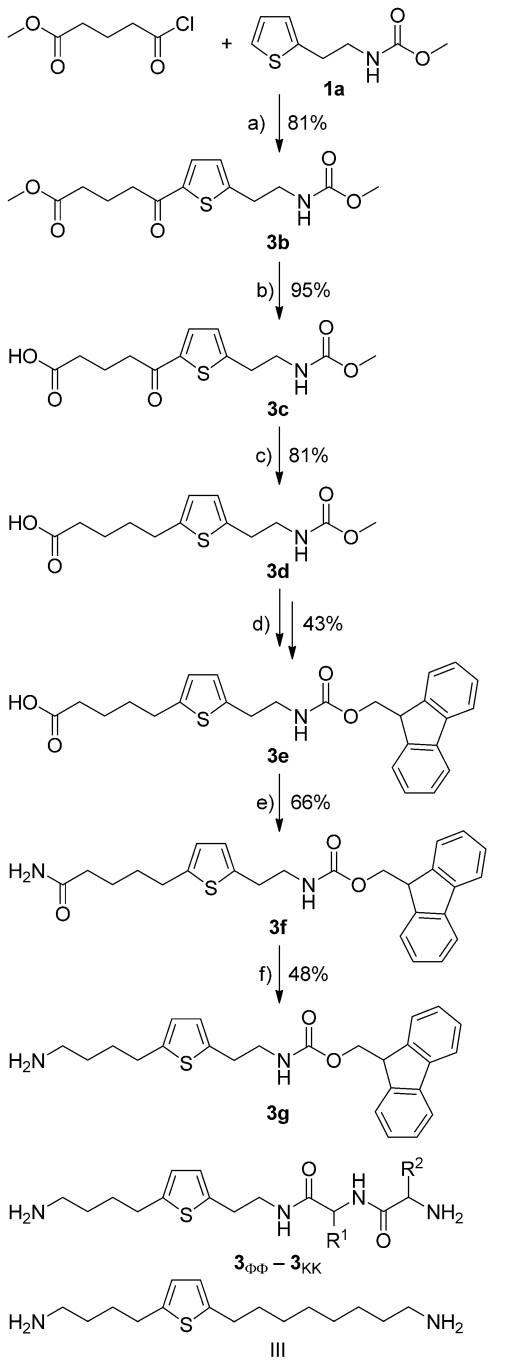

Scheme 2. Synthesis of the aminobutyl thienyl building block, allowing synthesis of $\mathbf{3}_{\underline{\Phi\Phi}}$–$\mathbf{3}_{\underline{KK}}$, structurally related to diamine **III**. *Reagents and conditions:* a) $AlCl_3$, DCE, 0 °C; 12 h, RT; b) LiOH, MeOH, H_2O, 12 h, RT; c) TFA/Et_3SiH, 12 h, 55–60 °C; d) 1. $N_2H_4{\cdot}H_2O$, KOH, ethylene glycol monoethyl ether, reflux, 1–1.5 h; 2. Fmoc-OSu, 2 N NaOH/dioxane, 12 h, RT; e) NHS, DCC, THF, 1 h, 0 °C; + NH_4HCO_3, 5 h, RT; f) trifluoroacetoxy iodobenzene, MeCN/H_2O (3:1), pyridine, 5 h, 60 °C.

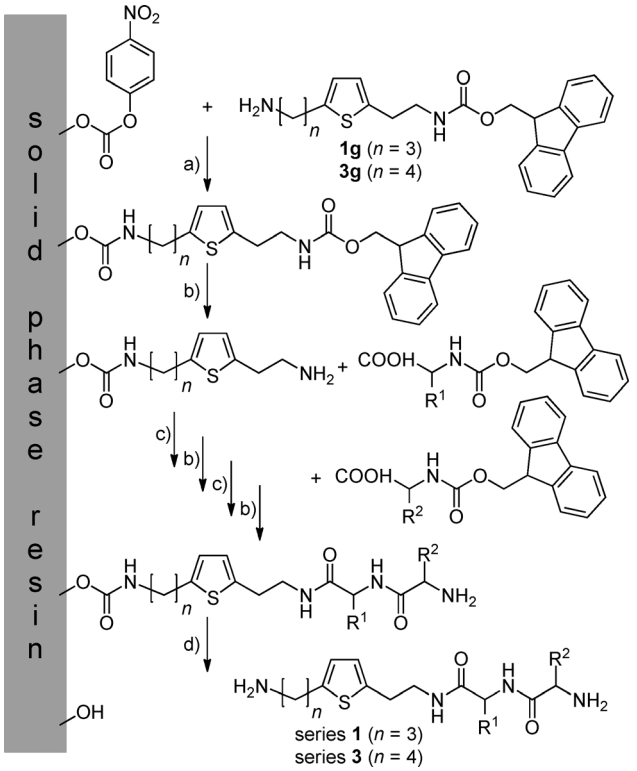

Scheme 3. Coupling of protected amino acids to immobilized building blocks **1 g** and **3 g**. Additional protection was required for some amino acids. *Reagents and conditions:* a) Abs THF, DIPEA, 14 h, RT; b) DMF, 40% piperidine, 2×20 min, RT; c) protected amino acid in DMF/DIC/HOBt, 3 h, RT; d) TFA/TIS/H_2O, 3 h, RT.

Inhibitory (dotted outline) and stimulatory effects (dark background) were more pronounced at low buffer concentration (10 mM, B; detailed data in table S5, Supporting Information). Strong inhibition was observed with compounds containing either Phe or (D)-Phe at both positions ($\mathbf{1}_{FF}$, $\mathbf{1}_{\underline{FF}}$, $\mathbf{1}_{\underline{FF}}$, $\mathbf{1}_{\underline{FF}}$). In contrast, pronounced stimulation was observed with compounds containing either Lys or (D)-Lys at both positions ($\mathbf{1}_{KK}$, $\mathbf{1}_{\underline{KK}}$, $\mathbf{1}_{\underline{KK}}$, $\mathbf{1}_{\underline{KK}}$).

The second and third series allowed an investigation of all aromatic amino acids in combination with each other. Here, the length of the free arm of the diamine building block was adjusted from three (as in N3T8N, **I**) to four methylene groups as in the more potent N4Ph8N (**II**) and N4T8N (**III**; see Schemes 1 and 2).[18] These compounds showed stronger inhibition (Figure 2) than the Phe analogues of the first series, most likely due to elongation of the free alkylamine arm (data in tables S9 and S11, Supporting Information).

Series **2** compounds with benzene in the diamine building block (Figure 2 A) acted slightly weaker than series **3.1** compounds with thiophene (panel B), reproducing the relation between N4Ph8N and N4T8N.[18] In terms of absolute potency, Trp was the most successful amino acid, especially at the second (outer) position (in agreement with Ferrer-Montiel et al.),[4] whereas compounds containing His did not show pronounced inhibition.

A final series **3.2** included all possible combinations of amino acids with positively charged residues Arg, His, and (D)-Lys; in addition, the adduct with (D)-Lys-Lys was prepared. As an initial overview, Figure 3 illustrates the influence of 10 μM test compound on [^{3}H]MK-801 binding (not 100 μM as in Figures 1 and 2). Most compounds containing at least one lysyl residue exhibited stimulation at this concentration (a phenom-

A)

	%	G	L	L	F	F	K	K
	G	81	82	90	76	76	89	79
	L	77	79	81	81	76	88	83
	L	91	91	85	81	85	93	92
aa1	F	78	68	60	58	55	90	84
	F	73	69	71	54	56	104	82
	K	94	103	94	89	82	121	112
	K	99	92	99	74	72	112	123

B)

	%	G	L	L	F	F	K	K
	G	65	69	88	40	65	131	100
	L	79	78	79	72	62	112	101
	L	77	82	81	67	68	96	105
aa1	F	36	44	50	45	36	84	83
	F	41	62	37	36	35	89	86
	K	117	118	114	86	77	173	145
	K	118	109	113	61	66	131	165

Figure 1. Influence of dipeptidic long-chain amines H_2N-$(CH_2)_3$-2,5-thiophene-$(CH_2)_2$-NH-aa$_1$-aa$_2$ (**1**$_{GG}$–**1**$_{KK}$, 100 μM) on [^{3}H]MK-801 binding to rat brain membranes (% specific binding), in A) high (50 mM) and B) low (10 mM) Tris buffer concentration; (D)-amino acids are underlined. Note that inhibitions (<100, minima outlined by dots) and stimulations (>100, dark background) are more pronounced at low buffer concentration (panel B). Full data are listed in Supporting Information table S5.

A)

	%	Φ	F	Y	W	H
	Φ	39	30	38	13	94
	F	33	20	26	13	56
aa1	Y	33	42	40	13	77
	W	32	26	27	10	55
	H	95	86	65	55	119

B)

	%	Φ	F	Y	W	H
	Φ	31	39	42	12	102
	F	31	12	21	12	49
aa1	Y	23	23	29	9	38
	W	34	5	12	4	39
	H	94	61	58	52	96

Figure 2. Influence of 100 μM dipeptidic long-chain amines A) H_2N-$(CH_2)_4$-1,4-phenyl-$(CH_2)_2$-NH-aa$_1$-aa$_2$ (**2**$_{ΦΦ}$–**2**$_{HH}$) and B) H_2N-$(CH_2)_4$-2,5-thiophene-$(CH_2)_2$-NH-aa$_1$-aa$_2$ (**3**$_{ΦΦ}$–**3**$_{HH}$) on [^{3}H]MK-801 binding to rat brain membranes (% specific binding); Φ: (D)-phenylglycine; minima outlined by dotted lines. Thieno analogues (panel B) consistently showed stronger inhibition than the corresponding phenyl analogues (panel A). Full data are listed in Supporting Information tables S9 and S11.

enon that would be missed at 100 μM; see Figure 5C,D below). Interestingly, Arg residues did not produce this stimulation. To our surprise, compound **3**$_{RH}$, with Arg at the first and His at the second position, turned out to be one of the most potent inhibitors of all (dotted frame in Figure 3).

	%	R	H	K	K
	R	84	63	116	
aa1	H	92	89	120	
	K	116	97	142	132

Figure 3. Influence of 10 μM dipeptidic long-chain amines H_2N-$(CH_2)_4$-2,5-thiophene-$(CH_2)_2$-NH-aa$_1$-aa$_2$ (**3**$_{RR}$–**3**$_{KK}$) on [^{3}H]MK-801 binding to rat brain membranes (% specific binding); K: (D)-Lys; minimum indicated by dotted lines, stimulation by dark background. Note that Arg alone does not afford stimulation, and that **3**$_{RH}$ is a powerful inhibitor. Full data are listed in Supporting Information table S13.

Closer examination of potent exponents of series 1

Inhibitory properties of series **1** analogues with Phe or (D)-Phe at both positions were studied with a range of concentrations. We obtained mean IC_{50} values from 84 μM (**1**$_{FF}$, with Phe at both positions) down to 35 μM (**1**$_{FF}$, with (D)-Phe at both positions; full data in table S6, Supporting Information). The polyamine agonist spermine (10 μM) had a non-uniform influence on these inhibitions (Figure 4). Displacement by **1**$_{FF}$ [-Phe-(D)-Phe] was shifted to the right by one order of magnitude, whereas that for **1**$_{FF}$ [-(D)-Phe-Phe] was shifted only by a factor of 2.4. The stimulatory compounds of the first series were more potent than the inhibitory ones. Compounds containing Lys or (D)-Lys as both amino acids exerted stimulation on [^{3}H]MK-801 binding with mean EC_{50} values from 3.5 to 5.8 μM; the mean degree of stimulation was 53–99% (full data in table S8, Supporting Information). The concentration dependence was steep, with Hill coefficients of ~2 (Figure 5A,B). Stimulation of [^{3}H]MK-801 binding by these double-lysyl derivatives resembled stimulation by other compounds with multiple positive charges.[12,23]

We studied the effects of two selected compounds on NMDA-induced currents in cultured hippocampal neurons. The double-lysyl compound **1**$_{KK}$ clearly potentiated currents at a holding potential of +60 mV (Figure 6A), whereas currents induced at −70 mV were rather inhibited (panel B), most likely due to voltage-dependent channel block, as often encountered with polyamines at the NR.[13] At the highest concentration used (800 μM), inhibition seemed to be balanced by potentiation (panel B). The longer chain homologue **3**$_{KK}$ had no effect when cells were voltage clamped at +60 (panel C), but strongly inhibited NMDA currents at −70 mV (panel D), again presumably because of voltage-dependent channel block.

It should be noted that binding data, unlike patch clamp recordings, are obtained in the absence of any potential; this may explain some of the discrepancies observed. Nevertheless, stimulation of currents by **1**$_{KK}$ agreed with strong binding stimulation, while in the case of **3**$_{KK}$ a more prominent part of inhibition was already apparent from the binding data. It may be concluded that inhibition by double-lysyl compounds depends on the length of the short arm (butyl more potent than

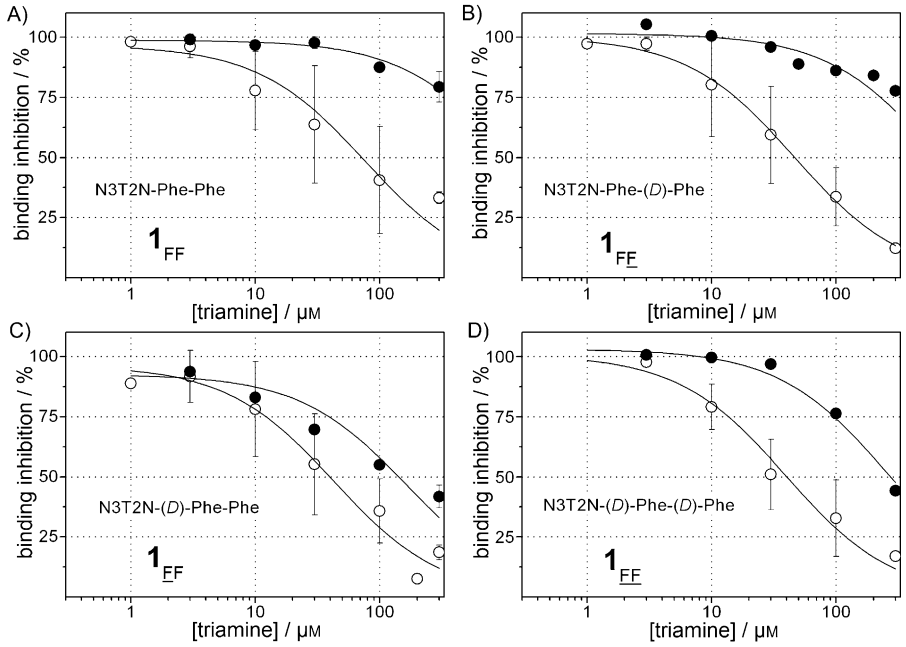

Figure 4. Inhibition of specific [^{3}H]MK-801 binding by dipeptidic long-chain triamines [N3T2N- is H_2N-$(CH_2)_3$-2,5-thiophene-$(CH_2)_2$-NH-] containing two Phe residues. Data are the mean ± SD pooled from A) nine, B) eight, C) nine, and D) eight experiments; circles without bars are the means of two results. Lines represent best fit to monophasic inhibition functions (Hill coefficient fixed to unity). ●: In the presence of 10 μM spermine, ○: without spermine. Note that the four compounds differ from each other in their sensitivity to spermine, not in absolute potency. Data are listed in Supporting Information table S6.

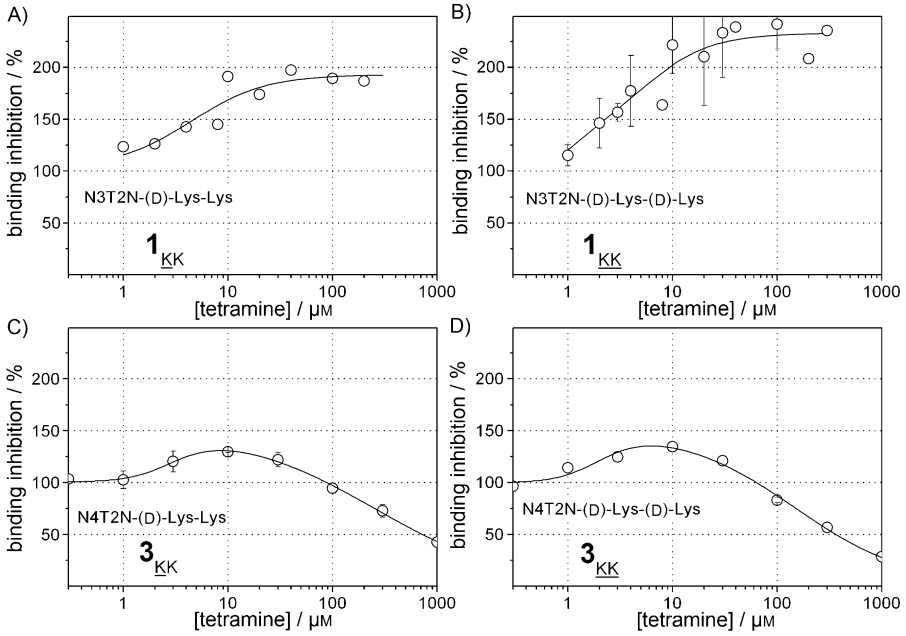

Figure 5. Influence of dipeptidic long-chain tetramines [N3T2N- is H_2N-$(CH_2)_3$-2,5-thiophene-$(CH_2)_2$-NH-, N4T2N- is H_2N-$(CH_2)_4$-2,5-thiophene-$(CH_2)_2$-NH-] with two Lys residues on specific [^{3}H]MK-801 binding. Data are the mean ± SD pooled from A) two, B) six, C) five, and D) five experiments; circles without bars are the means of two results. Lines represent best fit to monophasic saturation functions in panels A and B, and to biphasic functions in panels C and D. Note that all compounds stimulate at concentrations < 10 μM, but only the aminobutyl derivatives (panels C and D) provide inhibition at concentrations between 10 and 300 μM. Full data are listed in Supporting Information tables S8 and S15.

propyl); stimulation provided by the long dipeptidic arm was observed only if inhibition was weak.

The most challenging binding results were obtained with a mix of aromatic and basic amino acids. None of these compounds was remarkable at 100 μM (Figure 1), but their examination with multiple concentrations revealed biphasic concentration dependencies (Figure 7). Meticulous computational analysis of data pooled from several experiments revealed up to three components: two inhibitory and one stimulatory (Supporting Information table S7; the complexity of the data would allow other models as well). Common was inhibition at concentrations > 30 μM and a stimulatory component with a weaker EC_{50} value than observed for the double-lysyl compounds. This stimulation was hardly visible to the unaided eye; only $\mathbf{1}_{KF}$ demonstrated robust stimulation at 20–40 μM (Figure 7 A, ○). Here also a small inhibitory component appeared at similar concentrations. This high-affinity inhibitory component was eliminated with 1 μM spermine (Figure 7, ●).

The "FK compounds", with (L)- or (D)-Phe at the first and (L)- or (D)-Lys at the second position, yielded less spectacular results (figure S1, Supporting Information); a high-affinity inhibitory component was observed only in $\mathbf{1}_{FK}$, but not in the other three. The results obtained with mixed aromatic/basic compounds suggest that appropriately tailored agents should achieve partial inhibition of the NR, with inhibitory and stimulatory components counteracting each other. However, it can be expected that here as well (as shown above for some of the double-lysyl compounds), patch clamp recordings in cultured neurons would not yield exactly the same results.

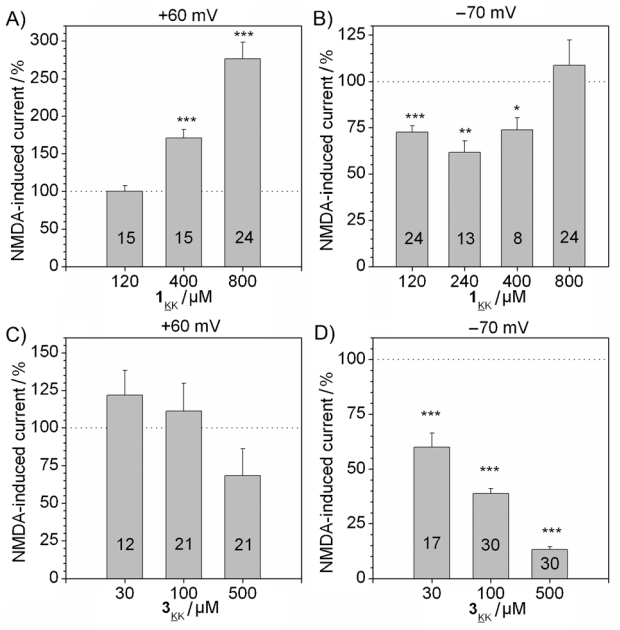

Figure 6. Influence of the double-lysyl compounds $\mathbf{1}_{KK}$ (A and B) and $\mathbf{3}_{KK}$ (C and D) on NMDA-induced currents (50 μM, in the presence of 10 μM glycine; mean ± SEM) in hippocampal cell cultures; pH 6.5 for A and B, pH 7.4 for C and D. Cells were from at least three different preparations; the number of cells is indicated in the bars; $*p < 0.01$, $**p < 0.001$, $***p < 0.0001$ (one sample *t*-test).

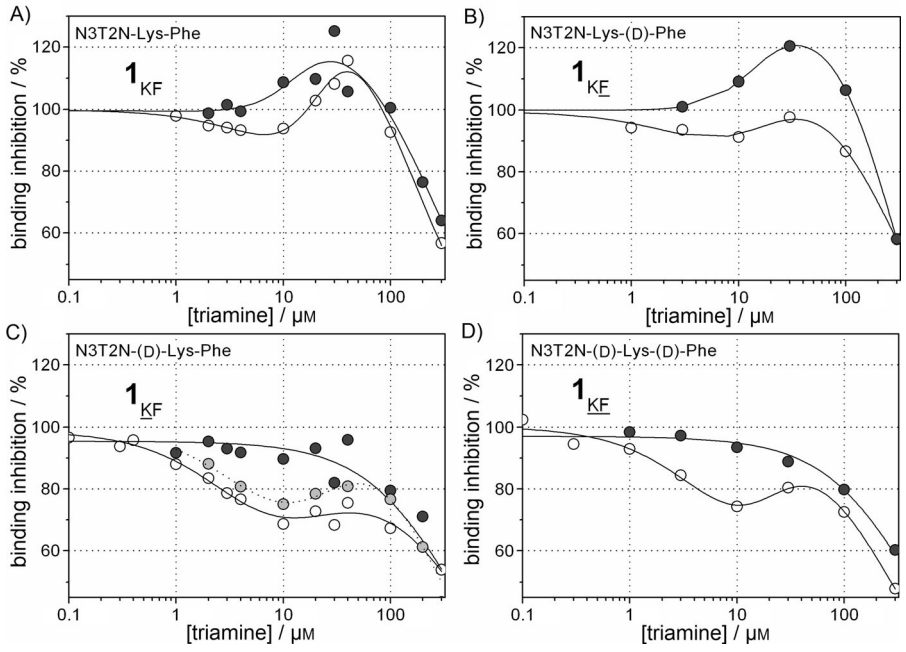

Figure 7. Influence of dipeptidic long-chain triamines [N3T2N- is H_2N-$(CH_2)_3$-2,5-thiophene-$(CH_2)_2$-NH-] containing one basic and one aromatic residue on specific [^{3}H]MK-801 binding (ordinate starts at 45%). Data are the mean pooled from A) six, B) two, C) twelve, and D) nine experiments. Lines represent best fit to functions presented in table S7 (Supporting Information). Filled circles illustrate the influence of spermine (● in C: 0.4 μM, ● in A, B, D: 1 μM). Note that inhibition by concentrations < 10 μM (especially in C and D) was eliminated by 1 μM spermine.

Closer examination of Series 3.1

Most members of series **3.1** allowed investigation of attenuating influences by spermine and pH. Because the stimulatory effect of spermine at the NR is known to be due to the relief of tonic proton inhibition at physiological pH,[24] we were interested in both influences. Four examples are illustrated in Figure 8. All four compounds exerted monophasic inhibition of [^{3}H]MK-801 binding. The double-Trp derivative $\mathbf{3}_{WW}$, the most potent inhibitor of this series, is shown in panel A (○). Spermine at 10 μM shifted the concentration dependence to the right by a mean factor of 4.7 (●; full data listed in table S12, Supporting Information). The other compounds in Figure 8 were less potent, but their potency was more sensitive to spermine; for the Tyr-Phe derivative $\mathbf{3}_{YF}$ (Figure 8B), the mean spermine shift factor was 11.3, for the double-Tyr derivative $\mathbf{3}_{YY}$ (panel C) it was 11.6, and for the Tyr-His derivative $\mathbf{3}_{YH}$ (panel D) it was 12.4. Interestingly, all these highly spermine-sensitive compounds contain Tyr in the first position.

Inhibition by the potent double-Trp derivative $\mathbf{3}_{WW}$ was modestly sensitive to pH changes (Figure 8A, triangles); the mean IC_{50} decreased from 15.1 μM at pH 7.0 to 8.6 μM at pH 6.4, and increased to 47.3 μM at pH 8.2 (full data in table S14, Supporting Information). An example for strong pH influence is the Tyr-His derivative $\mathbf{3}_{YH}$ (triangles in panel D): here, the IC_{50} value decreased from 62 μM at pH 7.0 to 13 μM at pH 6.4 (i.e., almost to the potency of $\mathbf{3}_{WW}$ at this pH), and increased to 566 μM at pH 8.2. Compounds such as $\mathbf{3}_{YH}$ represent a lead to therapeutics that exhibit their protective role at acidic pH (as in brain tissue suffering from ischemia).

Figures 9 and 10 summarize these relationships for most compounds of series **3.1** (only the weakest compounds could not be tested under attenuating conditions). Derivatives with Tyr at the first position were strongly influenced by 10 μM spermine (grey bars in Figure 9). A different picture emerged for pH influence (Figure 10). Here, four of the five most pH-sensitive compounds did contain His (grey bars, among them $\mathbf{3}_{YH}$ shown in Figure 8D), the fifth was the double-Tyr derivative $\mathbf{3}_{YY}$ (light grey in Figure 10; Figure 8C).

If compared directly with each other, both influences (spermine and pH) appear to be correlated (Figure 11). This correlation is due primarily to dipeptidyl polyamine analogues with positively charged residues His and/or Arg (●); together with the terminal primary amino groups, they expressed three to four positive charges. In compounds with neutral substituents (i.e., in diamines), spermine sensitivity seemed to vary without relation to pH influence. No such correlation had been de-

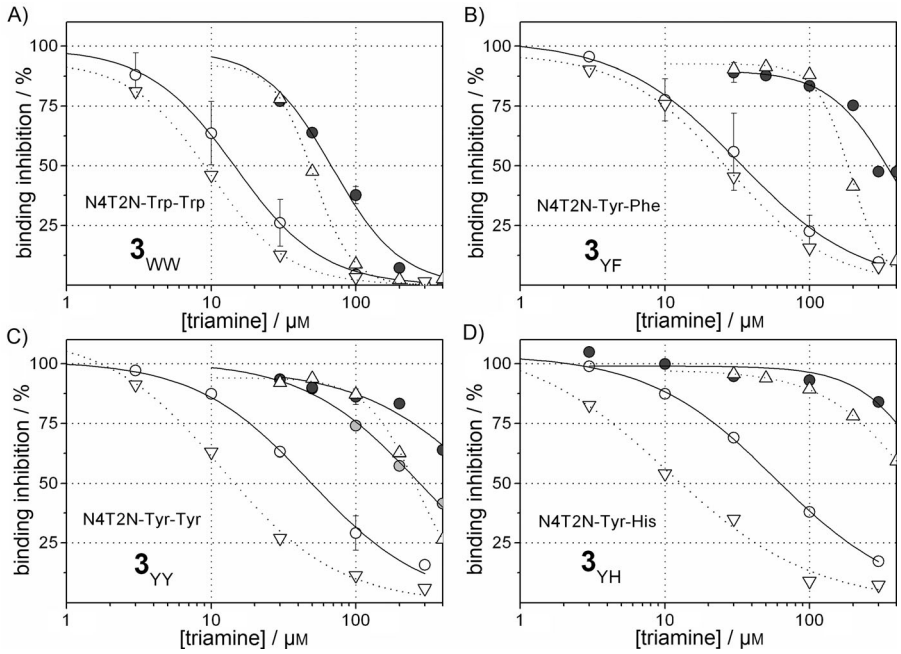

Figure 8. Inhibition of specific [^{3}H]MK-801 binding by dipeptidic long-chain triamines [N4T2N- is H_2N-$(CH_2)_4$-2,5-thiophene-$(CH_2)_2$-NH-] with various sensitivities to pH (▽: pH 6.4; △: pH 8.2) and spermine (● in C: 3 μM, ●: 10 μM); pH in control experiments was 7.0. Note that $\mathbf{3}_{YY}$ (panel C) and $\mathbf{3}_{YH}$ (panel D) were especially sensitive to pH and spermine.

scribed for derivatives of spermine and spermidine with aromatic substituents.[25]

Combination of positively charged residues

Finally, we synthesized a mini-library of $3\times3+1$ dipeptidic analogues with the longer butylamine arm, combining Arg, His, and D-Lys (series **3.2**). In addition to $\mathbf{3}_{\underline{KK}}$, we also prepared $\mathbf{3}_{K\underline{K}}$ (for comparison with the first series). As expected, these latter double-lysyl derivatives provided stimulation (grey background in Figure 3). Relative to the double-lysyl groups of the first series, they appeared to be of higher potency ($EC_{50}=2$ μM, full data listed in table S15, Supporting Information) than $\mathbf{1}_{\underline{KK}}$ and $\mathbf{1}_{K\underline{K}}$ (3.5 and 3.9 μM, table S8, Supporting Information). However, they did not stimulate to the same extent and exerted inhibition at lower concentrations than series **1** compounds (see Figure 5 C,D). Also in patch clamp experiments with $\mathbf{3}_{\underline{KK}}$ and hippocampal neurons, inhibition clearly surpassed stimulation (in contrast to

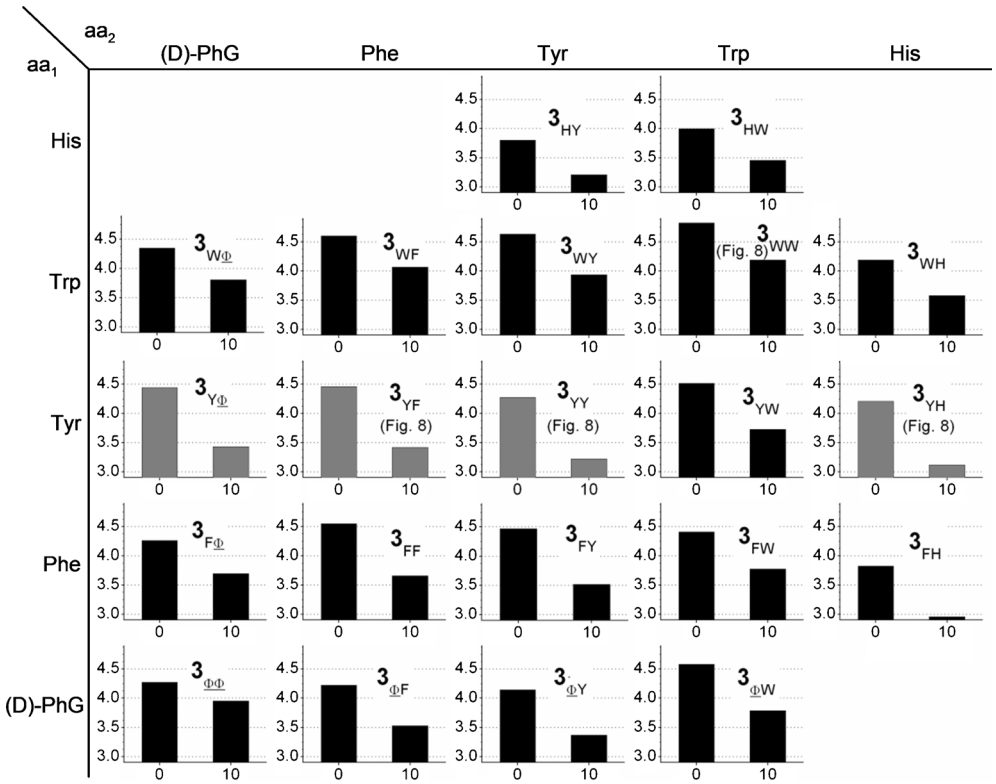

Figure 9. Influence of 10 μM spermine on inhibition of [^{3}H]MK-801 binding by dipeptidic compounds H_2N-$(CH_2)_4$-2,5-thiophene-$(CH_2)_2$-NH-aa_1-aa_2. Negative logarithms of IC_{50} values are plotted against spermine concentration (μM). Only 21 of 25 N4-thieno analogues are presented. Note that column height is significantly decreased by spermine, especially for compounds containing Tyr at the first position (grey bars). Data are shown in greater detail for some compounds in Figure 8; full data are listed in Supporting Information table S12.

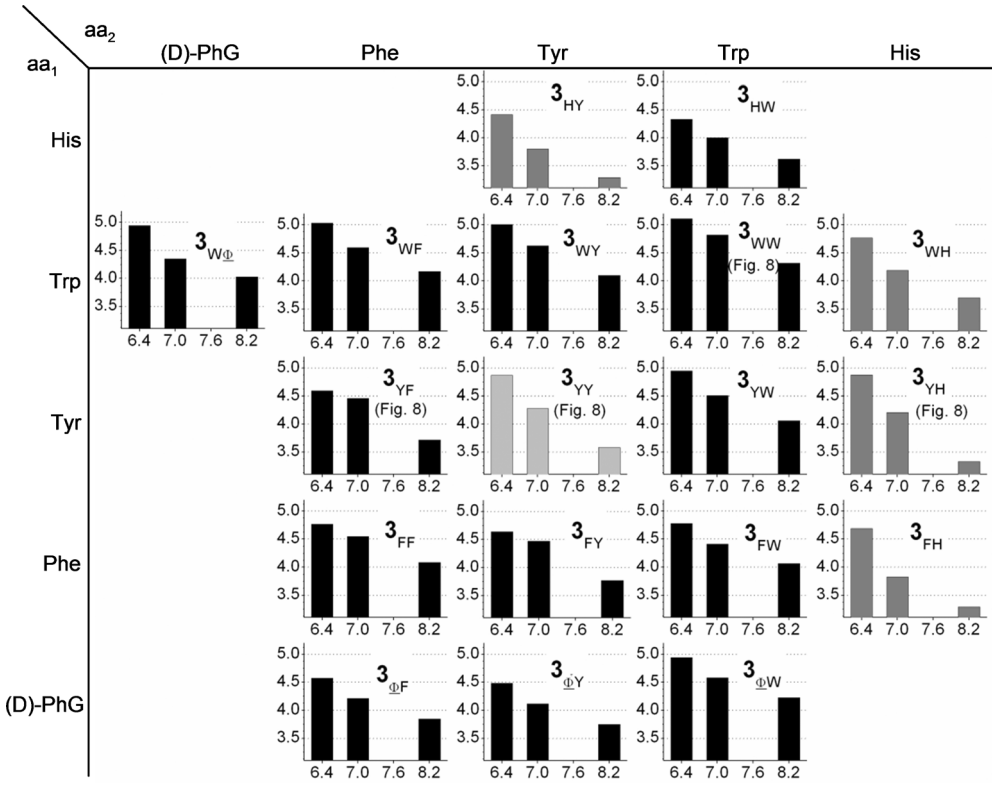

Figure 10. Influence of pH on the inhibition of [^{3}H]MK-801 binding by dipeptidic compounds H_2N-$(CH_2)_4$-2,5-thiophene-$(CH_2)_2$-NH-aa_1-aa_2. Negative logarithms of IC_{50} values are plotted against pH. Only 18 of 25 N4-thieno analogues were investigated in detail. Note that column height is significantly decreased with increasing pH, especially for the His-containing compounds $\mathbf{3}_{FH}$, $\mathbf{3}_{YH}$, $\mathbf{3}_{WH}$, and $\mathbf{3}_{HY}$ (grey bars), but also in the double-tyrosyl $\mathbf{3}_{YY}$ (light grey). Data are shown in greater detail for some compounds in Figure 8 and for all compounds in Supporting Information table S14.

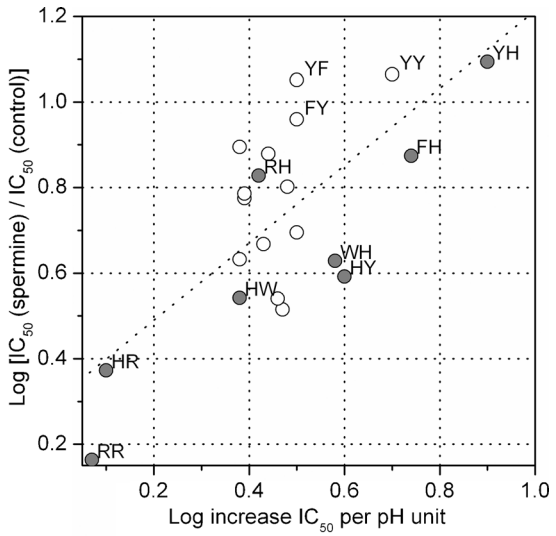

Figure 11. Influence of 10 μM spermine in relation to influence of pH. The logarithms of the IC_{50} ratios as illustrated in Figure 9 are plotted against the pH effects as illustrated in Figure 10. Note that the highest sensitivities to spermine are exhibited by compounds containing the dipeptides Tyr-Phe, Tyr-Tyr, and Tyr-His (●), compounds with positive charge. The dotted line indicates linear correlation ($r = 0.71$, $p < 0.001$).

$\mathbf{1}_{\underline{KK}}$; Figure 6). Compounds with only one (D)-Lys residue provided stimulation of binding to a similar level (+34 up to +48%), but with somewhat lower potencies (EC_{50} 5–6 μM; full data listed in table S15, Supporting Information). The inhibitory component in these single-lysyl derivatives was stronger (IC_{50} ~ 100 μM) than in the double-lysyl compounds (IC_{50} ~ 400 μM). Surprisingly, Arg was not able to step in for (D)-Lys or Lys. Even the double-arginyl compound $\mathbf{3}_{RR}$ provided only moderate inhibition at pH 7.0 without a visible stimulatory component (only at pH 6.4 did a stimulatory component appear; not shown). In this last library of compounds, we did not expect to find a potent inhibitor; nevertheless, $\mathbf{3}_{RH}$ came out as one of the most potent compounds of this study (IC_{50} 19.6 μM at pH 7.0; 9.4 μM at pH 6.4). Concerning its sensitivity to spermine and pH (●"RH" in Figure 11), it assumed an inconspicuous position amidst the double-aromatic adducts (○; data in tables S14 and S15, Supporting Information).

Structure–activity relationships

The facilitating influence of polyamines at the NR relies on structural requirements[12,23] that are to some extent mirrored by our results. Our most potent activators (the double-lysyl compounds) exhibit four positive charges on primary amino groups distal from each other. Single-lysyl derivatives with only three positive charges provided somewhat weaker stimulation (as spermidine with three charges is somewhat weaker than spermine with four). The failure of Arg to step in for Lys appears in line with the recently proposed mechanism of action: promoting closure of the lower lobe NTD dimer interface be-

tween the NR subunits GluN1 and GluN2B.[15] Planar six-membered rings formed by amidine/carboxy pairs[26] may not always allow the same extent of domain closure as a slim primary amino group.

While the observed EC_{50} values of our lysyl stimulators are in the range of known polyamine agonists, the IC_{50} values of even our most potent inhibitors (10–20 μM, depending on pH) are relatively weak in comparison with standard polyamine inverse agonists such as arcaine or 1,12-diaminododecane (5–10 μM).[23] Nevertheless, inhibitors with certain structural features exhibited pronounced sensitivity to spermine; the concentration–response curves for inhibitors of series **3.1** with Tyr in the first position ($\mathbf{3}_{YX}$, so to say; with the exception $X \neq W$) were shifted to the right by a factor of 10 with 10 μM spermine. Under our assay conditions, spermine resulted in half-maximal stimulation of [^{3}H]MK-801 binding at 1.97 ± 0.28 μM (with $h = 2.2 \pm 0.6$; mean ± SD, pooled from 29 experiments). Although these data are no proof, they would be compatible with a mechanism of inhibition by $\mathbf{3}_{YX}$ competitive with stimulation by spermine. This interaction would take place at the recently described lower lobe NTD dimer interface[15] with their pattern of acidic amino acid residues contributed by GluN1 and GluN2B. In fact, GluN2B contributes two Tyr residues to this interface, which might interact with partner residues contributed by GluN1, and $\mathbf{3}_{YX}$ might interfere at this target.

Although the main outcome of polyamine stimulation of the NR is relief from proton block,[24] this block is observed at all NR subtypes, but relief by polyamines depends on the GluN2B subunit. Thus, proton block and polyamine stimulation seem to be mediated by separate domains. Interestingly, we also observed different SARs for spermine and pH sensitivity of our compounds. To coin another abbreviation, epitomizing the pronounced pH influence of inhibitors $\mathbf{3}_{FH}$, $\mathbf{3}_{YH}$, and $\mathbf{3}_{WH}$, the typical compound with increased potency at acidic pH was $\mathbf{3}_{XH}$. A His residue appears well suited to mediate pH influences, with partial protonization at neutral pH.

Stimulatory and inhibitory influences appeared in combination in $\mathbf{1}_{KF}$, $\mathbf{1}_{\underline{K}F}$, $\mathbf{1}_{K\underline{F}}$, and $\mathbf{1}_{\underline{KF}}$. The inhibitory components appeared at lower IC_{50} values (in $\mathbf{1}_{K\underline{F}}$, $\mathbf{1}_{\underline{K}F}$, and $\mathbf{1}_{\underline{KF}}$; 5–11 μM) than in compounds exhibiting monophasic inhibition. Apparently, the positive charge of the lysyl residue not only conveyed positive intrinsic activity (observed as stimulation at medium concentrations), but also increased the negative influence of the phenyl group (observed as inhibition at low concentrations). Such cooperation may also explain the surprising potency of $\mathbf{3}_{RH}$; here, the charge was contributed by Arg, and the aromatic character by His. Because Arg lacks stimulatory properties, $\mathbf{3}_{RH}$ did not display the complex behavior of the "KF compounds", but only monophasic inhibition. Combinations of Arg with aromatics such as Phe, Tyr, or Trp should provide even stronger inhibition; this would be the subject of another library.

Conclusions

A diamine scaffold with an aromatic center was attached to a solid-phase resin and successfully functionalized with substituents of various sizes and physicochemical properties. Detailed dose–response relationships at the NR on rat brain membranes allowed the identification of inhibitory and stimulatory compounds; compounds with both aromatic and positively charged residues exhibited superposition of both properties. Inhibition of the NR by dipeptidic polyamine analogues was especially sensitive to spermine if a Tyr residue was present, whereas the presence of a His residue conferred high potency at acidic pH. Compounds with the latter property are of high therapeutic interest. Our compounds may serve as models for the development of therapeutic drugs and the elucidation of the polyamine regulatory site of the NR.

Experimental Section

General chemical procedures

NMR spectra were recorded on a Bruker spectrometer (^{1}H at 200–500, ^{13}C at 50–125 MHz). Chemical shifts (δ) are reported in ppm downfield from $(CH_3)_4Si$ ($\delta = 0$ ppm). The signal patterns are indicated as s, singlet; bs, broad singlet; d, doublet; t, triplet; q, quartet; qn, quintet; dd, double doublet; dt, double triplet; tt, triple triplet; m, multiplet. Melting points were determined with a Büchi 530 capillary-tube melting point apparatus and are not corrected. TLC was performed on silica gel (Merck 60 F_{254}); reaction products were visualized by UV fluorescence (λ 254 nm), by exposure to iodine vapor, or after spraying with 5% ethanolic molybdatophosphoric acid and subsequent heating. The products were purified by flash chromatography on silica gel 60 (70–200 mesh ASTM, 0.063–0.200 mm) purchased from Merck. Protected amino acid building blocks were commercially available in high purity (> 97%). Products from solid-phase synthesis were obtained in low quantities, therefore characterization by electrospray ionization mass spectrometry replaced NMR analysis; additionally, they were subjected to purity control by capillary electrophoresis (in 100 mM phosphate buffer at 25 °C, voltage 25 kV, 67/60 capillaries). Et_2O and THF were freshly distilled from sodium; DCE was distilled over phosphorous pentoxide; MeOH was distilled from magnesium methoxide; PE and CH_2Cl_2 were distilled before use. Abbreviations: EtOAc, ethyl acetate; AcOH, acetic acid; CE, capillary electrophoresis; Et_2O, diethyl ether; DIC, diisopropylcarbodiimide; DIPEA, diisopropylethylamine; Fmoc-OSu, Fmoc-*N*-hydroxysuccinimide; HOBt, 1-hydroxybenzotriazole (peptide coupling reagent); MeCN, acetonitrile; MeOH, methanol; NHS, *N*-hydroxysuccinimide; PE, petroleum ether; Et_3N, triethylamine.

Preparation of diamine building blocks

The following diamine building blocks, Fmoc protected at the amino group, were prepared as bridges between the Wang anchor of the resin and the dipeptides. 1) Compounds $\mathbf{1}_{GG}$–$\mathbf{1}_{\underline{K}\underline{K}}$ (series **1**; see Table 1) 3-[5-(2-aminoethyl)thien-2-yl]propylamine-Fmoc (**1 g**); 2) compounds $\mathbf{2}_{\Phi\Phi}$–$\mathbf{2}_{HH}$ (series **2**) 4-[4-(2-aminoethyl)phen-1-yl]butylamine-Fmoc (**2 g**); and 3) compounds $\mathbf{3}_{\Phi\Phi}$–$\mathbf{3}_{HH}$ and $\mathbf{3}_{RR}$–$\mathbf{3}_{\underline{K}\underline{K}}$ (series **3**) 4-[5-(2-aminoethyl)thien-2-yl]butylamine-Fmoc (**3 g**).[18] Synthesis of the diamine building block **3 g** is described below in detail (Scheme 2). Building blocks **1 g** and **2 g** were prepared in the same way as well (Scheme 1). Analytical details for these latter preparations can be found in the Supporting Information.

Synthesis of methyl *N*-[2-(2-thienyl)ethyl] carbamate (1 a): 2-(2-Thienyl)ethylamine (1 equiv) was dissolved in dioxane and aqueous NaOH (1.5 equiv); the methyl ester of chloroformic acid (1.1 equiv)

was dissolved in dioxane and added dropwise. After stirring overnight at RT the solvent was evaporated, the residue dissolved in saturated aqueous $KHSO_4$ and extracted three times with EtOAc. The organic layer was washed with brine, dried over Na_2SO_4, and purified by chromatography (PE/Et_2O 3:1, $R_f = 0.20$), giving 2.67 g (95%) **1a** as a pale-yellow liquid. ^{1}H NMR (300 MHz, $CDCl_3$): $\delta =$ 3.00 (t, $^3J = 6.6$ Hz, 2H, 2H-C(2)), 3.40–3.47 (dt as m, 2H, 2H-C(1)), 3.64 (s, $^3J = 6.6$ Hz, 3H, N-COOCH_3), 4.81 (s, 1H, NH), 6.81 (m, $^3J =$ 3.3 Hz, $^4J = 0.9$ Hz, 1H, 1H-C(3′)), 6.92 (dd, $^3J_1 = 5.0$ Hz, $^3J_2 = 3.4$ Hz, 1H, 1H-C(4′)), 7.14 ppm (m, $^3J = 5.1$ Hz, $^4J = 1.1$ Hz, 1H, 1H-C(5′)); ^{13}C NMR (50 MHz, $CDCl_3$): $\delta = 30.31$ (1C, 1C(2)), 42.34 (1C, 1C(1)), 52.04 (1C, N-COOCH_3), 123.87/125.31/126.96 (3C, 1C(3′), 1C(4′), 1C(5′)), 141.08 (1C, 1C(2′)), 156.87 ppm (1C, C=O); IR (KBr): $\tilde{\nu} = 3335$, 2946, 1697, 1537, 1454, 1144, 1032, 776, 704 cm^{-1}; Anal. calcd for $C_8H_{11}NO_2S$ [185.24 Da]: C 51.87, H 5.98, N 7.56, found: C 51.62, H 6.11, N 7.55.

Synthesis of methyl 5-(5-{2-[(methoxycarbonyl)amino]ethyl}thienyl)-5-oxopentanoate (3b): For synthesis of **3b** by Friedel–Crafts acylation (Scheme 2), **1a** was dissolved in dry DCE and added dropwise at 0 °C to a suspension of $AlCl_3$ (3.5 equiv) and glutaric acid monomethyl ester chloride (1.1 equiv) in dry CH_2Cl_2. After 12 h at RT, excess $AlCl_3$ was destroyed with 2 N HCl, and the product was extracted into CH_2Cl_2. After drying over $NaSO_4$ the solvent was evaporated, and the residue was purified by chromatography (PE/Et_2O 1:5, $R_f = 0.27$), giving 12.0 g (81%) **3b** as a white powder; mp: 60–61 °C; ^{1}H NMR (300 MHz, $CDCl_3$): $\delta = 2.04$ (q, $^3J = 7.1$ Hz, 2H, CH_2-(3″)), 2.42 (t, $^3J = 7.1$ Hz, 2H, CH_2-(2″)), 2.92 (t, $^3J = 7.2$ Hz, 2H, CH_2- (4″)), 3.04 (t, $^3J = 6.5$ Hz, 2H, CH_2-(2)), 3.45–3.47 (m, 2H, CH_2-(1)), 3.66/3.67 (2 s, 6H, 2×CH_3O), 6.85 (d, $^3J = 3.7$ Hz, 1H, 1H- C(3′)), 7.56 ppm (d, $^3J = 3.74$, 1H, 1H-C(4′)); ^{13}C NMR (50 MHz, $CDCl_3$): $\delta =$ 19.69 (C(3″)), 31.06 (C(2)), 32.98 (C(2″)), 37.67 (C(4″)), 41.93 (C(1)), 51.49 (CH_3OCO), 52.11 (CH_3OCONH), 126.69 (C(3′)), 132.27 (C(4′)), 142.59 (C(1′)), 150.73 (C(5′)), 156.83 (NHCOOCH_3), 173.52 (COOCH_3), 192.00 ppm (C(5″)O); Anal. calcd for $C_{14}H_{19}NO_4S$ [313.37 Da]: C 53.66, H 6.11, N 4.47, found: C 53.80, H 6.21, N 4.52.

Synthesis of 5-(5-{2-[(methoxycarbonyl)amino]ethyl}thienyl)-5-oxopentanoic acid (3c): LiOH (1.5 equiv) was added slowly to a solution of **3b** in MeOH/H_2O (50:1). After stirring for ~24 h at RT (and complete disappearance of the educt), MeOH was evaporated, and the residue was dissolved in H_2O and acidified with 2 N HCl. After exhaustive extraction with EtOAc, the organic layer was dried over Na_2SO_4, and the solvent was evaporated. The residue was purified by chromatography (CH_2Cl_2/MeOH 20:1, $R_f = 0.15$), giving 4.5 g (95%) **3c** as a pale-yellow powder; mp: 103–108 °C; ^{1}H NMR (300 MHz, MeOD): $\delta = 1.97$ (q, $^3J = 7.2$ Hz, 2H, CH_2-(3″)), 2.39 (t, $^3J =$ 7.3 Hz, 2H, CH_2-(2″)), 2.96–3.06 (m, 4H, CH_2-(4″)), 6.96 (d, $^3J =$ 3.8 Hz, 1H, 1H-C(3′)), 7.73 ppm (d, $^3J = 3.8$ Hz, 1H, 1H- C(4′)); ^{13}C NMR (50 MHz, MeOD): $\delta = 21.15$ (C(3″)), 31.75 (C(2)), 33.93 (C(2″)), 38.62 (C(4″)), 42.94 (C(1)), 52.48 (CH_3OCONH), 128.11 (C(3″)), 134.41 (C(4″)), 143.52 (C(5′)), 159.46 (C(2′)), 159.54 (CH_3OCONH), 176.87 (COOH), 194.63 ppm (C(5″)O); Anal. calcd for $C_{13}H_{17}NO_5S$ [299.34 Da]: C 52.16, H 5.72, N 4.68, found: C 52.23, H 5.63, N 4.67.

Synthesis of 5-(5-{2-[(methoxycarbonyl)amino]ethyl}thienyl)pentanoic acid (3d): For removal of the carbonyl oxygen, **3c** was stirred in 50 equiv TFA and 30 equiv Et_3SiH at 55–60 °C for 15 h. After addition of H_2O and acidification with $KHSO_4$, the product was extracted into EtOAc, the organic layer dried over Na_2SO_4, the solvent evaporated, and the residue purified by chromatography (CH_2Cl_2/MeOH 20:1, $R_f = 0.30$), giving 14.3 g (81%) of **3d** as a white powder; mp: 62–64 °C; ^{1}H NMR (300 MHz, MeOD): $\delta = 1.63$–1.65 (m, 4H, CH_2-(3″), CH_2- (4″)), 2.29 (t, $^3J = 6.8$ Hz, 2H, CH_2-(2″)), 2.75 (t, $^3J = 6.5$ Hz, 2H, CH_2-(5″)), 2.88 (t, $^3J = 7.2$ Hz, 2H, CH_2-(2)), 3.26–3.30 (m, 2H, CH_2-(1)), 3.60 (s, 3H, CH_3), 6.57–6.61 ppm (m, 2H, 1H-C(3′), 1H-C(4′)); ^{13}C NMR (50 MHz, MeOD) $\delta = 25.43$ (C(3″)), 30.62 (C(5″)), 31.31 (C(2)), 32.26 (C(4″)), 34.60 (C(2″)), 43.52 (C(1)), 52.42 (CH_3), 125.02 (C(4′)), 125.81 (C(3′)), 140.22 (C(5′)), 144.54 (C(2′)), 159.47 (NHCOOCH_3), 177.38 ppm (COOH); Anal. calcd for $C_{13}H_{19}NO_4S$ [285.36 Da]: C 54.72, H 6.71, N 4.90, found: C 54.86, H 6.73, N 4.97.

Synthesis of 9*H*-9-fluorenylmethyl *N*-{2-[5-(4-carboxybutyl)-2-thienyl]ethyl}carbamate (3e): For the synthesis of **3e**, the methyl carbamate protecting group had to be changed to an Fmoc protecting group. To achieve this, the old group was removed by Wolff–Kishner reduction, and the obtained free amine was treated further without isolation. Dissolved in ethylene glycol monoethyl ether, **3d** was held at reflux with 5 equiv $N_2H_4{\cdot}H_2O$ for 1–1.5 h. After addition of 3 equiv KOH, reflux was continued for another 3 h and the solvent evaporated. The residue was taken up in H_2O (bringing KOH to 2 N) and dioxane, and reacted further by slowly adding 1.1 equiv Fmoc-OSu dissolved in dioxane at RT. Stirring was continued for 12 h at RT, and dioxane was evaporated; the residue was distributed at 0 °C between 1 N HCl and EtOAc. The organic layer was dried over Na_2SO_4, the solvent evaporated, and the residue purified by chromatography (CH_2Cl_2/MeOH 20:1), giving 6.77 g (43%) **3e** as a white powder; TLC with PE/EtOAc/AcOH 1:1:1, $R_f =$ 0.35; mp: 97–99 °C; ^{1}H NMR (300 MHz, $CDCl_3$): $\delta = 1.70$ (m, 4H, CH_2-(3″), CH_2-(4″)), 2.36 (s, 2H, CH_2-(2″)), 2.77 (s, 2H, CH_2-(5″)), 2.95 (t, $^3J = 6.4$ Hz, 2H, CH_2-(2)), 3.41–3.47 (m, 2H, CH_2-(1)), 4.19–4.24 (m, 1H, 1H- C(9‴)), 4.39–4.48 (m, 2H, CH_2-fluorenyl), 4.93 (s, 1H, NH), 6.60 (s, 2H, 1H-C(3′), 1H-C(4′)), 7.30 (t, $^3J = 7.3$ Hz, 2H, 1H-C(2‴), 1H-C(7‴)), 7.40 (t, $^3J = 7.2$ Hz, 2H, 1H-C(3‴), 1H-C(6‴)), 7.58 (d, $^3J =$ 7.4 Hz, 2H, 1H-C(1‴), 1H-C(8‴)), 7.76 ppm (d, $^3J = 7.5$ Hz, 2H, 1H-C(4‴), 1H-C(5‴)); ^{13}C NMR (50 MHz, $CDCl_3$): $\delta = 24.07$ (C(3″)), 29.74 (C(5″)), 30.55 (C(2)), 30.91 (C(4″)), 33.68 (C(2″)), 42.33 (C(1)), 47.25 (C(9‴)), 66.66 (CH_2-fluorenyl), 119.98 (C(4‴), C(5‴)), 124.08/125.05 (C(3′), C(4′), C(1‴), C(8‴)), 127.03 (C(2‴), C(7‴)), 127. 68 (C(3‴), C(6‴)), 138.74 (C(4a), C(4b)), 141.32 (C(5′)), 143.59 (C(8a)), C(9a)), 143.92 (C(2′)), 156.33 (NHCOOCH_2-fluorenyl), 179.00 ppm (COOH); Anal. calcd for $C_{26}H_{27}NO_4S$ [449.56 Da]: C 69.46, H 6.05, N 3.11, found: C 69.70, H 6.03, N 3.28.

Synthesis of 9*H*-9-fluorenylmethyl *N*-{2-[5-(5-amino-5-oxopentyl)-2-thienyl]ethyl} carbamate (3f): To form the amide from carboxylic acid **3e**, the acid was stirred in absolute THF for 1 h at 0 °C together with 1 equiv NHS and 1.5 equiv DCC. After addition of aqueous NH_4HCO_3, the mixture was allowed to reach RT for ~5 h, THF evaporated, and the residue extracted with EtOAc. The organic layer was washed with 1 N HCl and with saturated $NaHCO_3$, and dried over Na_2SO_4. After filtration, the solvent was evaporated, and the residue was purified by chromatography (CH_2Cl_2/MeOH 20:1), giving 0.66 g (66%) **3f** as a white powder; TLC with EtOAc/PE 10:1, $R_f = 0.25$; mp: 145–146 °C; ^{1}H NMR (300 MHz, MeOD): $\delta =$ 1.64–1.72 (m, 4H, CH_2-(3″), CH_2- (4″)), 2.22 (t, $^3J = 6.8$ Hz, 2H, CH_2-(2″)), 2.78 (s, 2H, CH_2-(5″)), 2.95 (t, $^3J = 6.4$ Hz, 2H, CH_2-(2)), 3.41–3.45 (m, 2H, CH_2-(1)), 4.20–4.24 (m, 1H, 1H-C(9‴)), 4.39–4.41 (m, 2H, CH_2-fluorenyl), 4.99 (s, 1H, NHCOOCH_2-fluorenyl), 5.40 (s, 2H, NH_2), 6.60 (s, 2H, 1H-C(3′), 1H-C(4′)), 7.31 (t, $^3J = 7.1$ Hz, 2H, 1H-C(2‴), 1H-C(7‴)), 7.40 (t, $^3J = 7.3$ Hz, 2H, 1H-C(3‴), 1H-C(6‴)), 7.59 (d, $^3J = 7.3$ Hz, 2H, 1H-C(1‴), 1H-C(8‴)), 7.77 ppm (d, $^3J = 7.5$ Hz, 2H, 1H- C(4‴), 1H-C(5‴)); ^{13}C NMR (50 MHz, [D_6]DMSO): $\delta = 24.56$ (C(3″)), 29.64 (C(5″)), 30.47 (C(2)), 30.80 (C(4″)), 33.48 (C(2″)), 42.73 (C(1)), 47.76 (C(9‴)), 65.23 (CH_2-fluorenyl), 120.01 (C(4‴), C(5‴)), 124.19/125.08 (C(3′), C(4′), C(1‴), C(8‴)), 127.12 (C(2‴), C(7‴)), 127.54 (C(3‴), C(6‴)), 138.34 (C(4a), C(4b)), 140.82 (C(5′)), 143.51 (C(8a)), C(9a)), 143.81 (C(2′)), 156.35 (NHCOOCH_2-fluorenyl),

174.13 ppm ($CONH_2$); Anal. calcd for $C_{26}H_{28}N_2O_3S$ [448.58 Da]: C 69.62, H 6.29, N 6.24, found: C 69.87, H 6.42, N 6.44.

Synthesis of 9*H*-9-fluorenylmethyl *N*-{2-[5-(4-aminobutyl)-2-thienyl]ethyl} carbamate, TFA (3 g): Finally, the Fmoc-protected building block **3 g** was obtained from **3 f** by Hofmann rearrangement. At RT, 1.3 equiv [bis(trifluoroacetoxy)iodo]benzene was added to a solution of **3 f** in MeCN/H_2O (3:1). The mixture was slowly heated to 60 °C before adding 2 equiv pyridine. The solution turned lightly yellow and was stirred for another 4 h at the same temperature. After evaporation of MeCN, the residue was extracted with CH_2Cl_2, the organic layer dried with Na_2SO_4, the solvent evaporated, and the residue purified by chromatography (MeCN/H_2O 3:1), giving 3.44 g (48%) **3 g** as a yellow–ochre powder; TLC with CH_2Cl_2/MeOH 10:1, $R_f = 0.24$; mp: 91–93 °C; ^{1}H NMR (300 MHz, MeOD): $\delta = 1.65$ (s, 4H, CH_2-(2″), CH_2-(3″)), 2.72 (s, 2H, CH_2-(4″)), 2.78–2.91 (m, 4H, CH_2-(2″), CH_2-(1″)), 3.37–3.39 (m, 2H, CH_2-(1)), 4.16–4.20 (m, 1H, 1H-C(9‴)), 4.35–4.37 (m, 2H, CH_2-fluorenyl), 5.01 (s, 1H, N*H*COOCH_2-fluorenyl), 6.54 (s, 2H, 1H-C(3′), 1H-C(4′)), 7.28 (t, $^3J = 7.2$ Hz, 2H, 1H-C(2‴), 1H-C(7‴)), 7.38 (t, $^3J = 7.3$ Hz, 1H-C(3‴), 1H-C(6‴)), 7.55 (d, $^3J = 7.4$ Hz, 2H, 1H-C(1‴), 1H-C(8‴)), 7.74 (d, $^3J = 7.4$ Hz, 2H, 1H-C(4‴), 1H-C(5‴)), 7.93 ppm (s, 3H, NH_3); ^{13}C NMR (50 MHz, [D_6]DMSO): $\delta = 26.55$ (C(2″)), 27.91 (C(3″)), 28.81 (C(4″)), 29.78 (C(2)), 38.58 (C(1′)), 41.91 (C(1)), 46.73 (C(9‴)), 65.28 (CH_2-fluorenyl), 120.02/120.12 (C(4‴), C(5‴)), 124.17/124.70 (C(3′), C(4′)), 125.15 (C(1‴), C(8‴)), 127.28 (C(2‴), C(7‴)), 127.60 (C(3‴), 1C(6‴)), 138.98 (C(4a), C(4b)), 140.75 (C(5′)), 142.31 (C(8a), C(9a)), 143.98 (C(2′)), 156.04 ppm (NCOOCH_2-fluorenyl); MS: ESI$^+$ [$M+$H]: 421.3 Da, ESI [$M-$H]: 112.7 Da; Anal. calcd for $C_{27}H_{29}F_3N_2O_4S$ [534.60 Da]: C 60.66, H 5.47, N 5.24, found: C 60.39, H 5.52, N 5.16.

Addition of the aromatic diamine building blocks to the resin

All solid-phase synthesis steps were carried out in Cellpor filter-fitted polypropylene syringes filled with Wang resin and in silylated glass vessels. The resin was loaded with *p*-benzyloxybenzyl alcohol (1.07 mmol g^{-1}) anchor groups. Solid-phase synthesis started by activating the Wang resin in dry CH_2Cl_2 and an inert atmosphere at 0 °C. After addition of 2 equiv 4-methylmorpholine and 2 equiv 4-nitrophenyl carbonate, the mixture was stirred for 2 h at the same temperature. Stirring was continued for 12 h without cooling. Finally the resin was washed three times in dry DMF, three times in dry CH_2Cl_2 and dried in vacuo. The diamine building block (Fmoc protected at the shorter ethylamine arm) was added to the activated resin in dry THF as the TFA or HI salt. The uncharged amino group was exposed to the activated resin by dropwise addition of DIPEA (2 equiv) over 2 h at RT. Stirring was continued for 12 h at RT. After three washing cycles with CH_2Cl_2/MeOH/DIPEA, the Fmoc protecting group was removed with 40% piperidine in DMF.

Amino acid additions, Series 1: compounds $\mathbf{1_{GG}}$–$\mathbf{1_{\underline{KK}}}$: After several washing steps, one of the seven Fmoc-protected amino acids Gly, Leu, (D)-Leu, Phe, (D)-Phe, Lys, or (D)-Lys (the latter two also Boc protected at the side chain nitrogen atom) were coupled to the free amino group of the immobilized building block **1 g** in a mixture of DIC (3 equiv) and HOBt (3 equiv) in DMF (3 h). After Fmoc deprotection with a solution of 40% piperidine in DMF over two cycles of 20 min, another of the seven protected amino acids was coupled to the free amino group. Deprotection was repeated, and the resin was prepared for product release by washing three times with each of the following solvents: DMF, THF, CH_2Cl_2, MeOH, Et_2O. Product splitting in TFA/TIS/H_2O (95:2.5:2.5) yielded the dipeptidic derivatives H_2N-$(CH_2)_3$-2,5-thiophene-$(CH_2)_2$-NH-aa_1-aa_2. The identity of the end products was verified by CE and MS analysis.

Amino acid additions, Series 2: compounds $\mathbf{2_{\underline{\Phi\Phi}}}$–$\mathbf{2_{HH}}$: Among the amino acids to be coupled in this series, Tyr, Trp, and His required additional protection. The NH groups in Trp and His were protected by Boc, and the phenolic OH group in Tyr by 2-chlorotrityl. The first amino acid was coupled to the free amine group of the immobilized building block **2 g** in a mixture of DIC (3 equiv) and HOBt (3 equiv) in DMF (3 h). After Fmoc deprotection with a solution of 40% piperidine in DMF over two cycles of 20 min (only deprotecting the aliphatic amino group, not the heterocyclic NH in Trp and His), another of the five protected amino acids was coupled to the free amino group. The Tyr protecting 2-chlorotrityl was cleaved off with CH_2Cl_2/TIS/TFA (94:5:1) and the Fmoc group from the aliphatic amino function with 40% piperidine in DMF. Then the double-substituted building block was split from the resin by TFA/TIS/H_2O (95:2.5:2.5), also resulting in removal of the Boc groups and yielding the dipeptidic derivatives H_2N-$(CH_2)_4$-1,4-phenyl-$(CH_2)_2$-NH-aa_1-aa_2. The identity of the end products was verified by CE and by MS analysis.

Amino acid additions, Series 3.1: compounds $\mathbf{3_{\underline{\Phi\Phi}}}$–$\mathbf{3_{HH}}$: The same five amino acids as in series **2** were coupled in all possible combinations as described above, starting by adding the first protected amino acid to the free amino group of the immobilized building block **3 g**. The identity of the finally obtained dipeptidic derivatives H_2N-$(CH_2)_4$-2,5-thien-2-yl-$(CH_2)_2$-NH-aa_1-aa_2 was verified by CE and by MS analysis.

Amino acid additions, Series 3.2: compounds $\mathbf{3_{RR}}$–$\mathbf{3_{\underline{KK}}}$: Finally, the nine possible double additions of Arg, His, and (D)-Lys again to immobilized **3 g** were prepared. In addition, we attached (D)-Lys-Lys (for comparison with $\mathbf{1_{\underline{KK}}}$ of the first series). Side chains of Lys and His were obtained protected with Boc, that of Arg with 2,2,4,6,7-pentamethyl dihydrobenzofuran-5-sulfonyl (Pbf).

Binding experiments

Specific binding of [^{3}H]MK-801 [(17–25 Ci mmol^{-1}, ART-661, ARC Inc., St. Louis, MO (USA); NET-972, PerkinElmer Life Sciences Inc., Boston, MA (USA)] to rat brain membranes (prepared from hippocampus or from cerebral cortex) was performed as described.[16–18] Against widespread habits (non-equilibrium conditions, that is, incubation time 1 h or shorter, some researchers even prefer the nominal absence of glutamate and glycine), we selected conditions close to equilibrium (2 h incubation time at 23 °C in 50 mM Tris acetate pH 7.0, saturation with 10 μM glutamate and glycine). Non-specific binding was defined by binding of [^{3}H]MK-801 to closed channels, that is, without addition of the channel opening co-agonists glutamic acid and glycine, but with addition of their respective antagonists (D)-APV (10 μM) and 5,7-DCKA (1 μM; both from Tocris–Cookson). When it turned out that inhibition of [^{3}H]MK-801 binding by most of our test compounds was sensitive to Tris buffer, we switched from 50 to 10 mM Tris for the greater part of the experiments described herein; to maintain equilibrium conditions, incubation time was increased from 2 to 3 h. IC_{50} values were obtained by computer fitting the inhibition data to the function $B = B_o \times IC_{50}{}^h/(x^h + IC_{50}{}^h) + NB$, for which B is the amount of radioligand bound at various concentrations x of the (inhibitory) test compound, B_o the specific binding at $x = 0$, h the Hill coefficient, and NB the nonspecific binding. Concentration-dependent stimulation was fitted to the function $B = B_o + stim \times x^h/(x^h + EC_{50}{}^h) + NB$, in which *stim* is the extent of maximum stimulation (see the Supporting Information for more complex functions, table S7).

Electrophysiology

Hippocampi were dissected from postnatal (1–4 days old) rat pups following decapitation. The use of enzymes, the trituration protocol, and the culture conditions were similar to published procedures,[27] except that dissociated hippocampal neurons were plated onto polylysine-coated 35 mm tissue culture dishes (Nunc). We seeded 10000–15000 cells into 8 mm glass rings to confine the cells to the center of the culture dishes. Cells were routinely cultured at 5% CO_2 and 36.5 °C for 8–19 days in vitro (DIV) before use.

We used standard whole-cell patch clamp techniques as previously described.[28] Whole-cell currents were amplified, filtered, recorded, and analyzed using an Axopatch 200B amplifier, a Digidata 1320A digitizer/data acquisition system, and pClamp 10 software (all from Axon/Molecular Devices). Patch pipettes were filled with (mM): CsCl 140, $CaCl_2$ 0.5, EGTA 5, HEPES 10; adjusted to pH 7.2 with CsOH. Holding potential was either −70 or +60 mV. The bathing solution consisted of (mM): NaCl 140, KCl 6, $CaCl_2$ 1, glucose 20, HEPES 10, tetrodotoxin 0.001; adjusted to pH 7.4 or 6.5 with NaOH. NMDA, glycine, and test compounds were diluted from frozen stock solutions at the day of the recordings. Substances were applied by means of a DAD-12 superfusion system (ALA Scientific Instruments). Current densities in response to 50 μM NMDA (in the presence of 10 μM glycine) increased from 5 to 15 pA/pF from 9 to 19 DIV, respectively.

Acknowledgements

We thank Prof. Dr. Sigismund Huck (Medical University of Vienna) for his help with the patch clamp experiments. Students Katharina Blutsch and David Schweida contributed to the binding data. We thank Christa Edling and Bodo Lachmann for MS analyses and capillary electrophoresis.

Keywords: dipeptidic scaffolds · NMDA · polyamine regulatory site · receptors · solid-phase synthesis

[1] a) J. F. Cargill, M. Lebl, *Curr. Opin. Chem. Biol.* **1997**, *1*, 67–71; b) J. J. Parlow, R. V. Devraj, M. S. South, *Curr. Opin. Chem. Biol.* **1999**, *3*, 320–336.
[2] a) J. P. Kennedy, L. Williams, T. M. Bridges, R. N. Daniels, D. Weaver, C. W. Lindsley, *J. Comb. Chem.* **2008**, *10*, 345–354; b) T. Pöhler, PhD Thesis, Johann Wolfgang Goethe University, Frankfurt/Main (Germany), **2003**.
[3] E. H. F. Wong, J. A. Kemp, T. Priestly, A. R. Knight, G. N. Woodruff, L. L. Iversen, *Proc. Natl. Acad. Sci. USA* **1986**, *83*, 7104–7108.
[4] A. V. Ferrer-Montiel, J. M. Merino, S. E. Blondelle, E. Perez-Payà, R. A. Houghten, M. Montal, *Nat. Biotechnol.* **1998**, *16*, 286–291.
[5] K.-K. Tai, S. E. Blondelle, J. M. Ostresh, R. A. Houghten, M. Montal, *Proc. Natl. Acad. Sci. USA* **2001**, *98*, 3519–3524.
[6] N. A. Anis, S. C. Berry, N. R. Burton, D. Lodge, *Br. J. Pharmacol.* **1983**, *79*, 565–575.
[7] L. Nowak, P. Bregestovski, P. Ascher, A. Herbert, A. Prochiantz, *Nature* **1984**, *307*, 462–465.
[8] A. B. MacDermott, M. L. Mayer, G. L. Westbrook, S. J. Smith, J. L. Barker, *Nature* **1986**, *321*, 519–522.
[9] J. W. Johnson, P. Ascher, *Nature* **1987**, *325*, 529–531.
[10] R. W. Ransom, N. L. Stec, *J. Neurochem.* **1988**, *51*, 830–836.
[11] T. S. Sprosen, G. N. Woodruff, *Eur. J. Pharmacol.* **1990**, *179*, 477–478.
[12] a) K. Williams, C. Romano, P. B. Molinoff, *Mol. Pharmacol.* **1989**, *36*, 575–581; b) I. J. Reynolds, *J. Pharmacol. Exp. Ther.* **1990**, *255*, 1001–1007.
[13] a) D. M. Rock, R. L. MacDonald, *Mol. Pharmacol.* **1991**, *41*, 83–88; b) M. Benveniste, M. Mayer, *J. Physiol.* **1993**, *464*, 131–163.
[14] R. S. Zukin, M. V. L. Bennet, *Trends Neurosci.* **1995**, *18*, 306–313.
[15] L. Mony, S. Zhu, S. Carvalho, P. Paoletti, *EMBO J.* **2011**, *30*, 3134–3146.
[16] M. L. Berger, I. Seifriz, M. Letschnig, C. Schödl, C. R. Noe, *Neurosci. Lett.* **1992**, *142*, 85–88.
[17] M. L. Berger, C. Schoedl, C. R. Noe, *Eur. J. Med. Chem.* **1998**, *33*, 3–14.
[18] T. Pöhler, O. Schadt, D. Niepel, P. Rebernik, M. L. Berger, C. R. Noe, *Eur. J. Med. Chem.* **2007**, *42*, 175–197.
[19] K. Stromgaard, K. Andersen, P. Krogsgaard-Larsen, J. W. Jaroszewski, *Mini-Rev. Med. Chem.* **2001**, *1*, 317–338.
[20] S. Tomasi, M. Le Roch, J. Renault, J.-C. Corbel, P. Uriac, B. Carboni, D. Moncoq, B. Martin, J.-G. Delcros, *Bioorg. Med. Chem. Lett.* **1998**, *8*, 635–640.
[21] L. A. Carpino, H. Shroff, S. A. Triolo, E.-S. M. E. Mansour, H. Wenschuh, F. Albericio, *Tetrahedron Lett.* **1993**, *34*, 7829–7832.
[22] D. A. Pearson, M. Blanchette, M. L. Baker, C. A. Guindon, *Tetrahedron Lett.* **1989**, *30*, 2739–2742.
[23] M. L. Berger, C. R. Noe, *Current Topics in Medicinal Chemistry, Vol. 3*, Research Trends, Trivandrum, **2003**, pp. 51–64.
[24] S. F. Traynelis, M. Hartley, S. F. Heinemann, *Science* **1995**, *268*, 873–876.
[25] M. L. Berger, A. Y. Bitar, M. J. Waitner, P. Rebernik, M. C. O'Sullivan, *Bioorg. Med. Chem. Lett.* **2006**, *16*, 2837–3841.
[26] J. Singh, J. M. Thornton, M. Snarey, S. F. Campbell, *FEBS Lett.* **1987**, *224*, 161–171.
[27] M. Zeitelhofer, J. P. Vessey, Y. Xie, F. Tubing, S. Thomas, M. Kiebler, R. Dahm, *Nat. Protoc.* **2007**, *2*, 1692–1704.
[28] S. Boehm, S. Huck, M. Freissmuth, *J. Neurosci.* **1996**, *16*, 4596–4603.

Received: October 15, 2012
Published online on December 6, 2012